IPSJ Journal Vol. 1 No. 1 1–11 (Jan. 1960)

Regular Paper

An Extended Method of Higher-order Local Autocorrelation Feature Extraction for Classification of Histopathological Images

Hirokazu Nosato,[†1] Tsukasa Kurihara,[†2,*1]
Hidenori Sakanashi,[†1] Masahiro Murakawa,[†1]
Takumi Kobayashi,[†1] Tatsumi Furuya,[†2]
Tetsuya Higuchi,[†1] Nobuyuki Otsu,[†1]
Kensuke Terai[†3] and Nobuyuki Hiruta [†3]

In histopathological diagnosis, a clinical pathologist discriminates between normal tissues and cancerous tissues. However, recently, the shortage of clinical pathologists is posing increasing burdens on meeting the demands for such diagnoses, and this is becoming a serious social problem. Currently, it is necessary to develop new medical technologies to help reduce their burdens. Therefore, as a diagnostic support technology, this paper describes an extended method of HLAC feature extraction for classification of histopathological images into normal and anomaly. The proposed method can automatically classify cancerous images as anomaly by using an extended geometric invariant HLAC features with rotation- and reflection-invariant properties from three-level histopathological images, which are segmented into nucleus, cytoplasm and background. In conducted experiments, we demonstrate a reduction in the rate of not only false-negative errors but also of false-positive errors, where a normal image is falsely classified as an image with an anomaly that is suspected as being cancerous.

1. Introduction

Currently, in histopathological diagnosis, a clinical pathologist makes diagnoses of normal or lesional tissue based on the microscopic observation of a histopathological specimen taken from a patient. Such diagnoses are of crucial importance in determining the most appropriate treatment for a patient. In diagnosing a life-threatening cancer, it is essential that the histopathological diagnosis is conducted accurately.

However, recently, because of a serious shortage in the number of clinical pathologists within Japan, the huge burdens that are being placed on working clinical pathologists have become an issue of public concern. As of December 31st, 2008, there were only 1,374 clinical pathologists, representing just 0.5% of all medical doctors[1)]. Moreover, pathologists who are 50 years old or older accounted for nearly 55% of the total, and so many of them will reach their mandatory retirement age within a dozen years or so[1)]. It is anticipated that the problem of aging pathologists will dramatically add to the shortage of clinical pathologist.

Since 1998, in Japan, the number of patients newly-diagnosed as having cancer is more than 500,000 each year[2)]. In 2004, they reached approximately 650,000, which is approximately three times the number for 1974[3)]. Accordingly, the increased demand for histopathological diagnosis associated with the rising numbers of cancer patients is placing additional burdens on working clinical pathologists. Besides, the shortage of pathologist can lead to serious problems, such as inaccurate diagnoses and diagnosis failures. Thus, it is a crucial issue to develop new medical technologies to help reduce their burdens, as there are as yet no prospects of solving the fundamental shortage of pathologists.

Some automatic diagnostic support methods for histopathological diagnosis have been developed by applying image recognition techniques. Various studies of automatic cancer diagnostic support based on histopathological micrographs have involved three steps, such as image preprocessing, feature extraction, and automatic classification[4)]. Such conventional technologies use morphological features extracted from the individual cells and nuclei which are clipped during preprocessing. Cossato, Miller, Graf and Meyer have proposed a technique of grading nuclear pleomorphism for histopathological micrographs[5)]. They clip nuclei from histopathological micrographs with hematoxylin-eosin (H-E) staining, and can classify cancerous nuclei according to some morphological features of the nucleus, such as area, diameter, and color shading, by using support vector machine (SVM) learning.

However, in these conventional methods, clipping accuracy has a huge impact

†1 National Institute of Advanced Industrial Science and Technology (AIST)
†2 Department of Information Science, Toho University
†3 Department of Surgical Pathology, Toho University Sakura Medical Center
*1 Presently with NEC Soft Ltd.

on the accuracy of the classification. When a histopathological image includes tissue artifacts, such as crushed tissue due to excessive force from tissue forceps and/or uneven staining, it is impossible to clip the cells and the nuclei with accuracy. Accordingly, the morphological features cannot be extracted appropriately for automatic classification. In the paper by Cossato et al.[5], only 70% of the nuclei were clipped with the correct contour, with 30% of the nuclei being unclipped and thus excluded from the feature extraction process. Naturally, if there were cancerous nuclei within the excluded portion, they would not be classified as anomaly. On the other hand, a clinical pathologist can diagnose histopathological specimens even when they include such artifacts. It is difficult to realize a technique of automatic classification for all the cells and nuclei within histopathological image based on conventional methods that involve the clipping process and the morphological model-based featre extraction.

In order to overcome these problems, we have proposed histopathological diagnostic support method[6] using higher-order local autocorrelation (HLAC) features[7]. Using this method, histopathological images that might be cancerous are classified as anomaly without clipping the cells and nuclei. However, the method had scope for improvement because it yielded considerable levels of false-positive errors, where a normal image would incorrectly be classified as an anomaly image. In this paper, in order to improve our histopathological diagnostic support method, we propose an extended method of HLAC feature extraction for classification of histopathological images. In our previous work[6], the general 25-dimentional HLAC features are simply extracted from the binarized histopathological images. In contrast, based on the perspectives that the pathologists pay attention to the aspects of tissue, and a histopathological image has no directional property, the extended method was developed to extract HLAC features with rotation- and reflection-invariant properties from three-level histopathological images, which are segmented into nucleus, cytoplasm and background.

In conducted experiments using histopathological images of gastric biopsies taken from patients, we demonstrate automatic image classification of histopathological images into normal and cancer with high accuracy and a reduction in the number of the false-positive results.

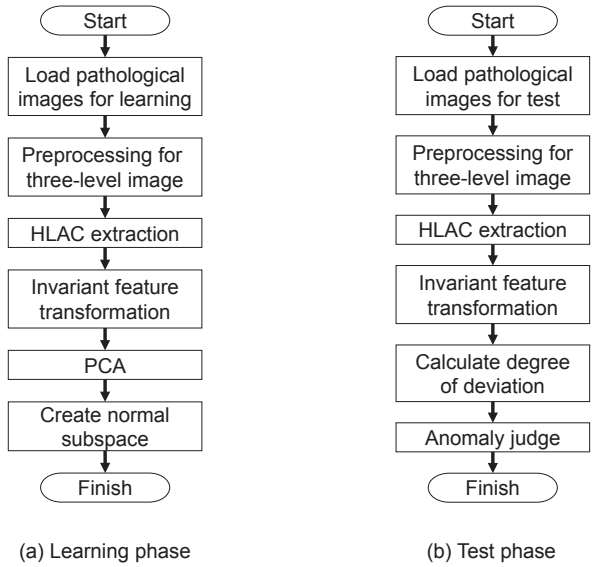

Fig. 1 Flowchart of proposed method.

2. Proposed method

An overview of the proposed process flow is shown in Fig.1. The proposed method consists of two phases, which are the learning phase (as shown in Fig.1(a)) and the test phase (as shown in Fig.1(b)). We detail the principal procedures of the proposed method below.

2.1 Three-level image

A histopathological image with H-E staining consists principally of the nucleus (blue), the cytoplasm (red) and the background (non-stained). A clinical pathologist can recognize the nucleus and the cytoplasm in terms of their coloring and shading, and they reason holistically by utilizing information about the nuclear area and its diameter, the nuclear-cytoplasmic ratio, the regularity of histopathological tissue and so on. There, in this paper, we focus only on information of the nucleus and cytoplasm and incorporate their importance for diagnosis into the our classification technology. At first, we segment a histopathological image

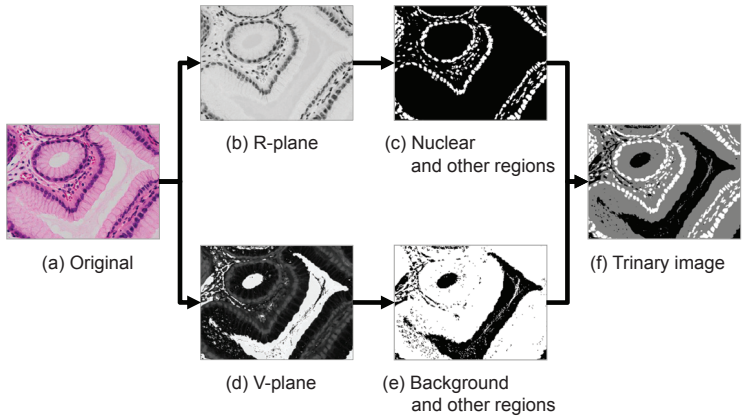

Fig. 2 Trinary histopathological images generated within the proposed method.

into three regions of the nuclei, the cytoplasm and the background, as shown in Fig.2. Next, we assign three levels to each region according to their respective importance for diagnosis.

2.1.1 Region segmentation

(1) Nuclear region

From pre-experimental results, it was discovered that the nuclear region is significantly different in terms of the R-plane (Fig.2(b)) compared to the other regions with the RGB color space. Accordingly, in this paper, we apply binarization with the Otsu method[8] to R-plane of a histopathological image to segment into the nuclear region. As a result, Fig.2(c) shows a binarized image with the nuclei (white) and the other regions (black).

(2) Background region

A background region without staining is white in color with the highest levels of brightness but it does not have any color information. In contrast, non-background region, including the nuclei and the cytoplasm, are mainly stained red color. Thus, we segment into the background region by using V-plane (Fig.2(d)), which represents the difference between red and brightness in the YUV color space. In this paper, we apply binarization with the Otsu method[8] to V-plane of a histopathological image to segment into the background region. As a result, Fig.2(e) shows a binarized image with the background (black) and the other regions (white).

(3) Image synthesis

We synthesize a trinary image from these two binarized images. Fig.2(f) shows a trinary histopathological image with the nucleus (white), the cytoplasm (gray) and the background (black).

2.1.2 Assignment of three levels

Instead of pixel values, we defined the level values for each region of trinary histopathological images. In this paper, we conducted a preliminary experiment to identify the optimal nuclear level under the fixed conditions of background level = 0 and cytoplasm level = 2, because information relating to the nucleus is most important for histopathological diagnosis. Fig.3 presents the preliminary experimental results which show the rates of false-positive errors, as described in detail in 3.2 below, for normal tissue images across a range of nuclear levels ($2 \sim 20$). Based on these results, we adopt 14 as the nuclear level with the minimum number of false-positive errors. Accordingly, the three levels of the nucleus, the cytoplasm and the background are 14, 2 and 0, respectively.

2.2 HLAC feature extraction

A general HLAC features[7] show geometrical features, such as area, contour and shape of the input image, according to the local autocorrelation as shown in Fig.4. In this paper, the HLAC features can be extracted as geometrical features of nucleus and cytoplasm by the proposed three-level image.

Each component of the HLAC features is formulated by the following autocorrelations:

$$g_N = \sum_r f(r) f(r + a_1) \cdots f(r + a_N) \tag{1}$$

where f is an three-level image of the target histopathological image, r is a position vector and a_i $(i = 1, \cdots, N)$ are the displacement vectors. These vectors are two-dimensional vectors within the image data, whose coordinates are $x - y$.

The number N represents the order of the HLAC, and this paper adopts $N = 0, 1, 2$. When the local displacement is restricted around r, a configuration of 3×3 pixels forms 35 local mask patterns which take the shift-invariant property into consideration, as shown in Fig.4. In each mask, "black" represents the pixels

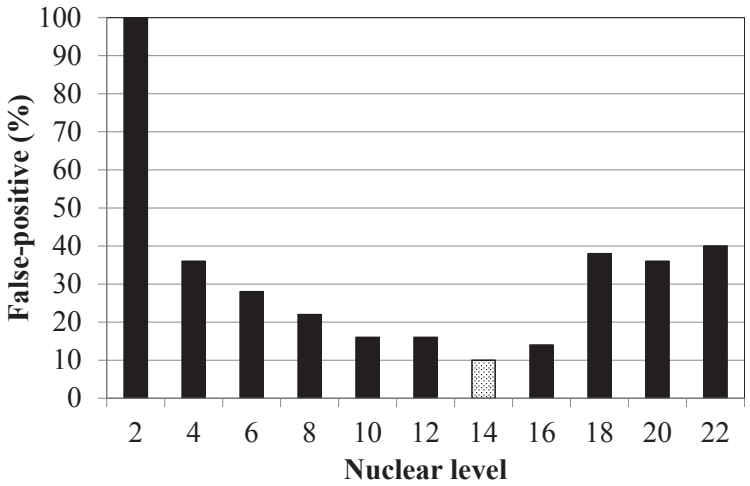

Fig. 3 Preliminary experimental result.

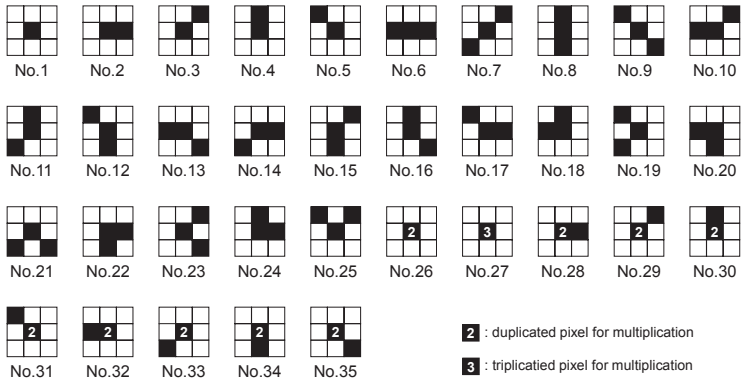

Fig. 4 HLAC patterns up to the 2nd order of correlation.

worked on multiplication while "white" represents "don't care". Thus, HLAC feature vectors are 35-dimensional vectors g_i $(i = 1, \cdots, 35)$ calculated according to the 35 patterns.

In this paper, we combine some set of HLAC feature vectors according to larger mask patterns, as shown in Fig.5, to extract more features from larger regions, because a pathologist observes histopathological specimens under a microscope with multiple viewing fields. A small field is used to observe an individual cell or nucleus. On the other hand, a wide field is used to assess the regularity of histopathological tissue. A variable w, as shown in Fig.5, represents the mask size. For example, if four values for w are used in extraction, the combined HLAC feature vectors g_{whole} will have 140-dimentional vectors.

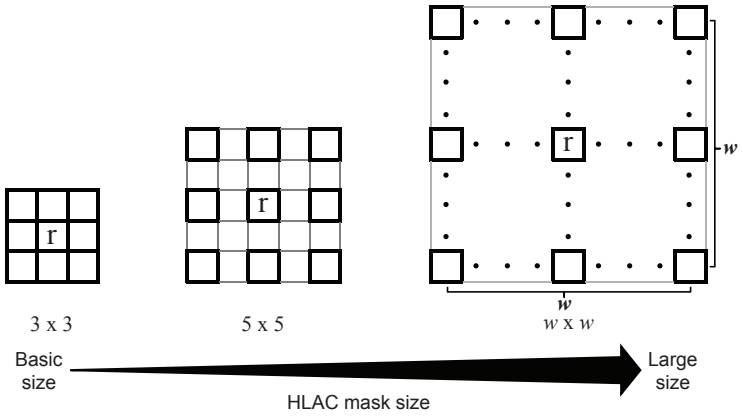

Fig. 5 HLAC mask image and expanded mask.

2.3 Invariant feature transformation

Because a histopathological image has no features in terms of the property of direction, such as vertical, horizontal and rotation directions, and no heads-tails differences, the HLAC features are extended to include rotation- and reflection-invariant properties. The extended HLAC feature vectors z_i $(i = 1, \cdots, 8)$ are reconfigured for 8-dimentional vectors with unification of some features as a single invariant feature according to Table 1. In this reconfiguration, we consider a rotation-invariant property with a $\pi/4$ rotation that can be designed by the 3×3 pixel mask, because a cell and a nucleus in a histopathological image form a rounded tissue. For example, the mask No. 6 as shown in Fig.4 is rotational symmetry of the mask No. 7, 8 and 9. Accordingly, their features total one invariant feature z_3, as shown in table 1.

Table 1 Invariant HLAC feature transformation.

Invariant HLAC feature	Basic HLAC feature (mask No.)
z_1	g_1
z_2	$g_2+g_3+g_4+g_5$
z_3	$g_6+g_7+g_8+g_9$
z_4	$g_{10}+g_{11}+g_{12}+g_{13}+g_{14}+g_{15}+g_{16}+g_{17}$
z_5	$g_{18}+g_{19}+g_{20}+g_{21}+g_{22}+g_{23}+g_{24}+g_{25}$
z_6	g_{26}
z_7	g_{27}
z_8	$g_{28}+g_{29}+g_{30}+g_{31}+g_{32}+g_{33}+g_{34}+g_{35}$

2.4 PCA and normal subspace

This paper calculates the base vectors forming the normal subspace by applying Principal Component Analysis to the HLAC feature vectors z_i extracted from normal tissue images. In this calculation, the eigenvectors $U = [u_1, \cdots, u_M]$, $u_i \in V^M$ $(i = 1, \cdots, M)$ are calculated by solving the following eigenvalue problem:

$$R_z U = U\Lambda,$$
$$R_z \triangleq E_{i=1}^{n}\{z_i z_i^T\} \tag{2}$$

where z_i $(i = 1, \cdots, M)$ are the M-dimensional feature vectors and $\Lambda = diag(\lambda_1, \cdots, \lambda_M)$ is the eigenvalue matrix. The variable order K forming the normal subspace is defined in terms of the contribution rate η_K as follows:

$$\eta_K = \frac{\sum_{i=1}^{K}\lambda_i}{\sum_{i=1}^{M}\lambda_i} \tag{3}$$

In this paper, the normal subspace is formed by the eigenvectors $U_K = \{u_1, \cdots, u_K\}$ as base vectors, according to the order K to satisfy the contribution rate $\eta_K \geq 0.999$, for example.

2.5 Anomaly judge

The projection operator for the normal subspace is given by $P = U_K U_K^T$. Then, the projection operator for the ortho-complement subspace to the normal subspace is given by $P_\perp = I_M - P$. The distance $d_\perp$ between an input feature vector z for a test image and the normal subspace is formulated as

$$d_\perp^2 = ||P_\perp z||^2 = z^T(I_M - U_K U_K^T)z \tag{4}$$

In this paper, we define $d_\perp$ as the anomaly value which is index to classify the images, as shown in Fig.6.

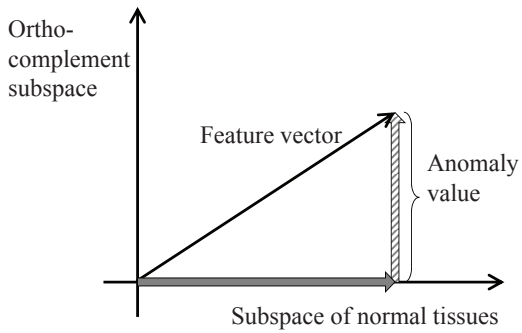

Fig. 6 Anomaly value.

3. Verification experiments

This paper conducted two verification experiments for the three-level image and the rotation- and reflection-invariant properties employed in the proposed method.

3.1 Test data for experiments

In the experiments, we used histopathological images (Fig.7) of the gastric biopsy taken from patients that had been classified as representing normal tissue and cancerous tissue by clinical pathologists.

In general, gastric biopsy samples treated by the pathologists were collected from the patients who are in variant conditions, such as early or end stage of cancer, suspected to be cancerous and might be normal (medical examination). Moreover, in many cases, because cancer area is not expanded all over the biopsy tissue, normal area can be cut out as images. Therefore, the pathologists can collect not only cancerous tissues but also normal tissues through the clinical routine work. In this paper, all the normal images were collected and diagnosed as normal by the clinical pathologists.

Table 2 presents the conditions of data set for the experiments. In this paper, 250 samples of normal tissue are used as the learning data. And then, another 50 samples of normal tissue and 24 samples of cancerous tissue are used as the

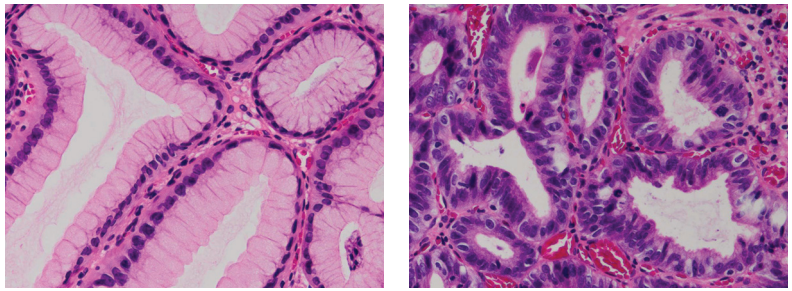

(a) Normal tissue image (b) Cancerous tissue image

Fig. 7 Histpathological images of gastric biopsy.

Table 2 Experimental data.

Data type	Diagnosis	Number of sample
Learning data	Normal	250
Test Data	Normal	50
	Cancer	24

test data. These histopathological images for the experiments were taken with microscopy of 20 times power and saved in 1280 x 960 JPEG color format.

3.2 Evaluation method for verification

In the experiments, the average μ and the standard deviation σ of the anomaly values $d_\perp$ of the learning data were calculated, and then $\mu + \sigma$ (which we refer to as "$H_{1\sigma}$") and $\mu + 2\sigma$ (which we refer to as "$H_{2\sigma}$") were set as the threshold that discriminates normal and anomaly. When the anomaly value $d_\perp$ for a test data exceeded these threshold values, it was classified as an anomaly that might be cancerous in nature. For the verifications, we counted the number of false-positives (FP) where a normal image was mistakenly classified as being an anomaly. In addition, we also counted the number of false-negatives (FN), where a case of cancerous tissue is not correctly classified as such.

3.3 Experimental result 1

This experiment was conducted to verify the effectiveness of the proposed three-level image. We used two conventional methods for comparison. They are gray-scale preprocessing and binary preprocessing implemented with the Otsu method[8]. This binary preprocessing was used to our previous method[6]. In the case of binary image, HLAC features are 25-dimentional vectors. Because a binary image consists of 0 and 1, the results of multiplication for the duplicated pixel and the triplicated pixel equal 1 (e.g. 1 x 1 = 1, 1 x 1 x 1 = 1). That is, about the HLAC masks as shown in Fig.4, No. 26 = No. 1, No. 27 = No.1, No.28 = No.2 and so on. Therefore, the HLAC features extracted from binary image are 25-dimentional vectors without No.26-No.35 masks.

Table 3 presents the experimental conditions of the proposed method and the two comparison methods. In this experiment, we used four values of the mask size w, specifically, 29, 33, 57 and 65, but the HLAC features were not extended to include the rotation- and reflection-invariant properties. Besides, in the every method, we used 0.99999 as the threshold for the contribution rate.

Fig.8 presents the original histopathological image, the two conventional images and the proposed three-level image (we assign Nuclei: 255, Cytoplasm: 127, Background: 0). The gray-scale image (Fig.8(b)) is the nearest to the original image (Fig.8(a)) and the tissue structure can be clearly seen. In the binary image (Fig.8(c)), many of the cytoplasm regions are intermingled with the background region. On the other hand, with the proposed three-level images (Fig.8(d)), the three regions of the nucleus, the cytoplasm and the background can be distinguished.

Table 4 shows evaluations for the three methods. For the gray-scale image, there were false-negatives according to both thresholds. In contrast, the other two methods yielded no false-negatives. The proposed method yielded the best performance in terms of false-positives in comparison to the other methods. As shown in Fig.9, the proposed method can classify cancerous samples as anomaly with larger margins of classification than the gray-scale result. And then the

Table 3 Experimental conditions.

Image	Number of gradation	HLAC features	Level
Gray-scale	255	140 (35×4)	$0 \sim 255$
Otsu binary	2	100 (25×4)	1 or 0
Proposed three-level	3	140 (35×4)	Nucleus:14, Cytoplasm:2, Background:0

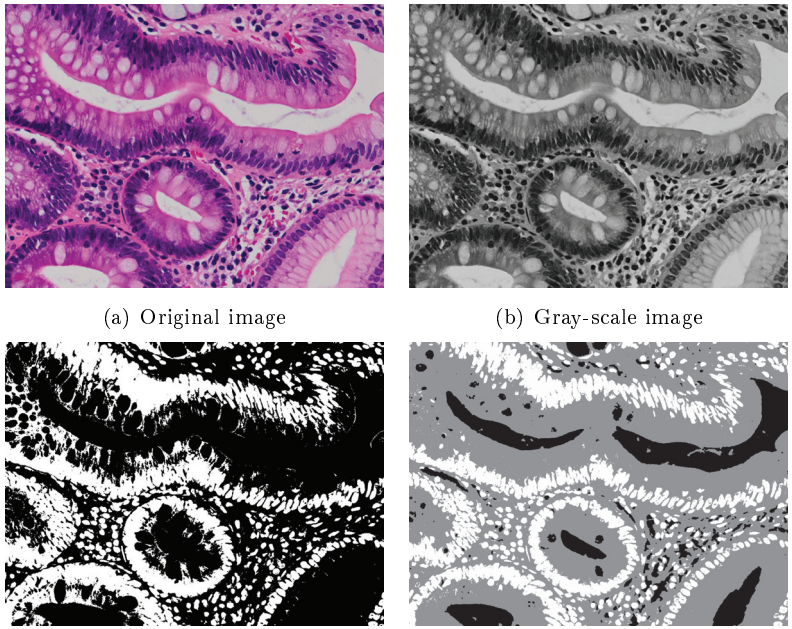

(a) Original image (b) Gray-scale image

(c) Otsu binary image (d) Proposed three-Level image

Fig. 8 Preprocessed histopathological images of gastric biopsies.

Table 4 Results of false-positive and false-negative for experiment 1.

Preprocessing	FP/FN for threshold H			
	$H_{1\sigma}$		$H_{2\sigma}$	
	FP	FN	FP	FN
Gray-scale	13	1	2	6
Otsu binary	43	0	33	0
Proposed three-level	28	0	16	0

proposed method can reduce the anomaly value of normal samples compared with the result of binary image regarded as our previous method.

3.4 Experimental result 2

This experiment was conducted to verify the effectiveness of the proposed invariant properties. We compare the results for the extended HLAC features with

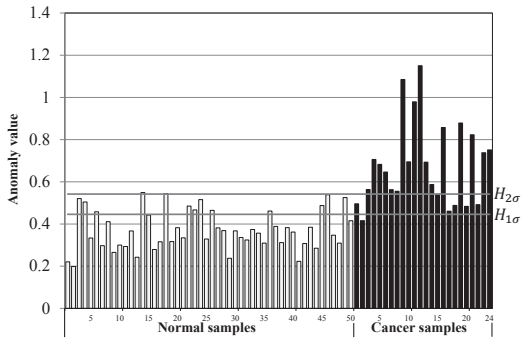

(a) Result of gray-scale images

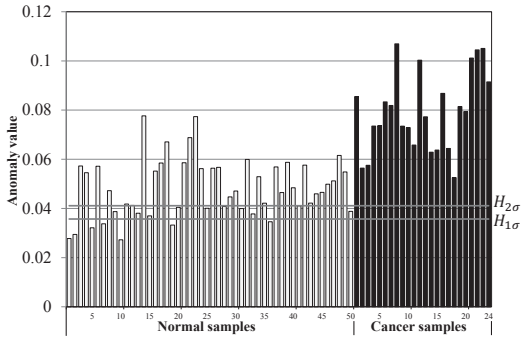

(b) Result of binary images

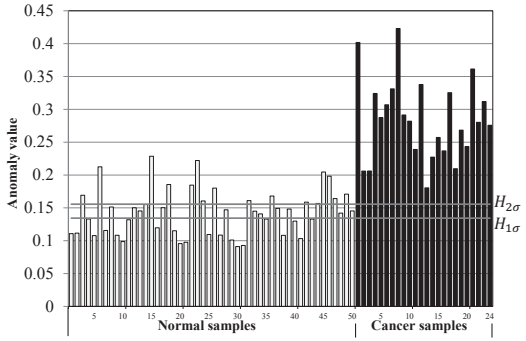

(c) Result of proposed three-level images

Fig. 9 Experimental results 1.

Table 5 Results of false-positive and false-negative for experiment 2.

HLAC	HLAC features	FP/FN for H			
		$H_{1\sigma}$		$H_{2\sigma}$	
		FP	FN	FP	FN
basic HLAC	140	28	0	16	0
extended HLAC	32	11	0	1	0

the results for the basic HLAC features using proposed three-level images. In this experiment, we used same conditions, which are the mask size w and the threshold for the contribution rate, as experiment 1. The HLAC feature vectors were 32-dimentional vectors and 140-dimentional vectors, respectively.

Table 5 presents the improvement in the number of false-positive due to the proposed invariant method. Fig.10 shows histograms of the anomaly values for normal images and cancerous images. Comparing the two panels, it is clear to see that the area of overlap between normal and cancerous samples is smaller for the extended HLAC features than for the basic HLAC feature. This result indicates that the proposed method is capable of classifying cancerous images as anomaly with greater accuracy and so considerably reduces the rate of false-positive errors.

4. Conclusion

This paper has proposed an extended method of HLAC feature extraction for image classification of histopathological images to improve our histopathological diagnostic support technology. The extended method can preprocess images to create three-level histopathological images, which are segmented into nucleus, cytoplasm and background. Moreover, the extended method also extracts HLAC features with rotation- and reflection-invariant properties from the three-level image. In conducted experiments using histopathological images for gastric biopsy taken from patients, we demonstrated automatic classification of histopathological images into normal and caner with high accuracy and reduction in the rate of not only false-negative errors but also of false-positive errors.

Although this paper used two types of samples that had been classified by pathologists, there are actually five classes of gastric biopsy tissue based on cell morphology and atypism. In order to advance towards the practical application of our proposed methods, additional studies on clinical classification will be needed.

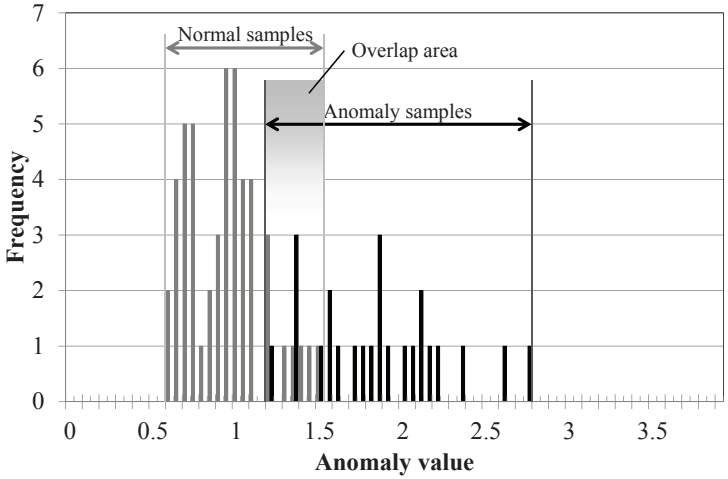

(a) Results of the basic HLAC

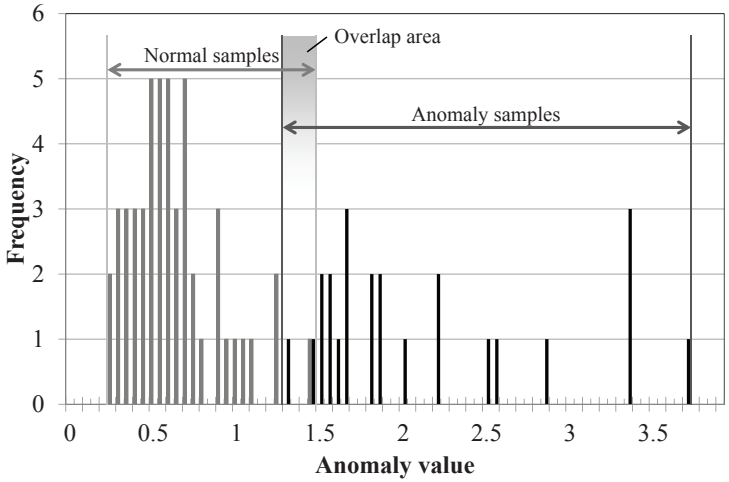

(b) Result of proposed invariant HLAC

Fig. 10 Frequency distribution graph of experimental results.

However, the basic scheme underlying our support technology can be applied to other type of medical imaging technology, such as endoscopy and computerized tomography. Thus, our method represents a key for solving shortages in medical staff in the future. Our proposed method can realize reductions in the burdens placed on medical staff. Accordingly, their increased opportunities to concentrate on the diagnosis of more problematic samples will contribute to achieving more accurate and more prompt medical treatment.

References

1) Statics and Information Department.: Survey of Physicians, Dentists and Pharmacists 2008. Ministry of Health, Labour and Welfare, (2010).
2) Matsuda, T., Marugame, T., Kamo, K., Katanoda, K., Ajiki, W., Sobue, T., and The Japan Cancer Surveillance Research Group.: Cancer incidence and incidence rates in Japan in 2003: based on data from 13 population-based cancer registries in the Monitoring of Cancer Incidence in Japan (MCIJ) project, Japanese Journal of Clinical Oncology, vol.39, pp.850–8, (2009).
3) Statics and Information Department.: Vital Statistics in JAPAN, Ministry of Health, Labour and Welfare, (2010).
4) Demir, C. and Yener, B.: Automated cancer diagnosis based on histopathological images: a systematic survey, Technical Report, TR-05-09, Rensselaer Polytechnic Institute, Mar. (2005).
5) Cosatto, E., Miller, M., Graf, H. P. and Meyer, J. S.: Grading Nuclear Pleomorphism on Histological Micrographs, Proc. of the 19th International Conference on Pattern Recognition (ICPR2008), pp.1-4, Tampa, USA, Dec. (2008).
6) Nosato, H., Sakanashi, H., Masahiro, M., Higuchi, T., Otsu, N., Terai, K., Hiruta, N. and Kameda, N.: Histpathological Diagnostic Support Technology using Higher-order Local Autocorrelation Features, Proc. 2009 International Symposium on Bio-Inspired, Learning, and Intelligent Systems for Security BLISS2009, pp.61–65, Edinburgh, United Kingdom, Aug. (2009).
7) Otsu, N. and Kurita, T.: A new scheme for practical flexible and intelligent vision systems, Proc. IAPR Workshop on Computer Vision, pp.431–435, Tokyo, Japan, Oct. (1988).
8) Otsu, N.: A threshold selection method from gray level histograms, IEEE Trans. Syst. Man & Cybern., vol.9, No.1, pp.62–66. (1979).
9) Nanri, T. and Otsu, N.: Unsupervised Abnormality Detection in Video Surveillance, Proc. IAPR Conf. on Machine Vision Application (MVA2005), pp.574-577, Tsukuba, Japan, May. (2005).

(Received November 10, 2010)
(Accepted August 1, 2011)

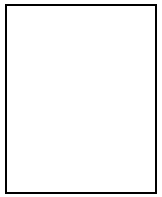

Hirokazu Nosato received the B.S. degree in chemistry, and M.S. and Ph.D. degrees in information science from Toho University, Chiba, Japan, in 1998, 2000 and 2003, respectively. He is currently a Researcher at National Institute of Advanced Industrial Science and Technology (AIST), Tsukuba, Japan. He is also an associate professor at the cooperative graduate school of Toho University. His research interests include optimization algorithm, pattern recognition, and their applications. He is a member of Information Processing Society of Japan.

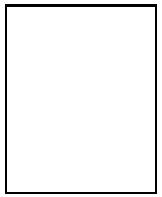

Tsukasa Kurihara received the B.S. and M.S. degrees in information science from Toho University, Chiba, Japan, in 2009 and 2011, respectively. His research interests include cluster analysis, medical image recognition, and color space conversion. He is currently working for NEC Soft Ltd.

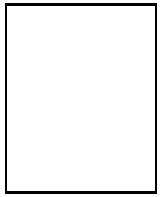

Hidenori Sakanashi received his Dr.Eng. degree in information engineering from Hokkaido University, Japan, in 1996. From 1996 to 1998 he was a fellow researcher of Japanese Society for the Promotion of Science (JSPS). In 1998, he joined National Institute of Advanced Industrial Science and Technology (AIST), Japan, where he is currently a senior researcher. His research interests include pattern recognition, image processing, evolutionary computation, and their applications. He is a member of Information Processing Society of Japan.

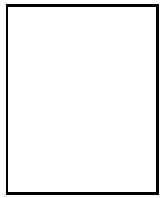

Masahiro Murakawa received his B.E., M.E., and Ph. D. degrees in mechano-informatics engineering from the University of Tokyo, Tokyo, Japan, in 1994, 1996, 1999, respectively. He heads the Smartgrid research group of information technology research institute, National Institute of Advanced Industrial Science and Technology (AIST), Tsukuba, Japan. He is also an associate professor at the cooperative graduate school of University of Tsukuba and Toho University. His research interests include optimization algorithms, adaptive systems, and adaptive learning. Dr. Murakawa received the best paper award at the second international conference on evolvable systems in 1998, the Tsukuba Encouragement Prize for 2000, the IEEJ millennium best paper award in 2001.

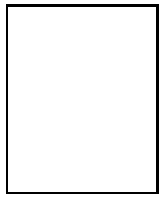

Takumi Kobayashi received master of engineering from University of Tokyo in 2005, and doctor of engineering from University of Tsukuba in 2009. He received the PRMU Award in 2008 for excellence in his research and the Best Paper Award from the Institute of Electronics, Information and Communication Engineers (IEICE) in 2010. His current research interests are pattern recognition, multivariate analysis, and their applications to image processing.

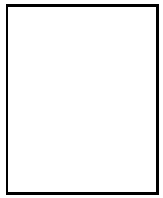

Tatsumi Furuya is a Professor in Information Science at Toho University. Prior to that, he worked at the AIST by 1994. He received Ph.D. from Seikei University. His research interests include image processing and human interface.

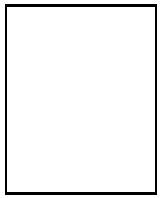

Tetsuya Higuchi belongs to AIST and he has worked in the area of Genetic Algorithms, Evolvable Hardware, PLC. He is also the professor of the University of Tsukuba. He received Ph.D. from Keio University. His recent research interests include pattern recognition and its practical applications.

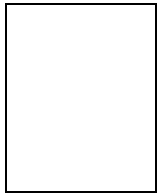

Nobuyuki Otsu received B.S., Mr. Eng. and Dr. Eng. in Mathematical Engineering from University of Tokyo in 1969, '71, '81, respectively. He joined ETL (now AIST) in 1971 and has been engaged in theoretical research and its application of pattern recognition, image processing, and multivariate analysis. From 2001 he has been AIST Fellow and also Professor at University of Tsukuba from 1992 to 2010 and at University of Tokyo from 2001 to 2007.

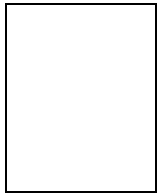

Kensuke Terai received his B.S. degree in chemistry from Toho University, Chiba, Japan, in 1996. He works in the Department of Surgical Pathology, the Department of Research and Development and the Department of Clinical Laboratory at Toho University Sakura Medical Center. He is also a Chief Medical Technologist and a Healthcare Information Technologist (certified by JAMI). He currently engages in pathological examination, genetic research, and medical care information system.

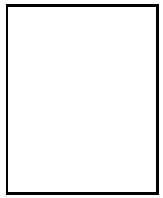

Nobuyuki Hiruta received his M.D. and Ph.D. degrees in faculty of medicine from Toho University, Tokyo, Japan in 1985 and 1993, respectively. From 1985 to 1992, he was an Assistant Professor of 1st Department of Pathology in School of Medicine, Toho University. Since October 1985 until April 1986, he had worked for the orthopedic surgery at Cancer Institute Hospital. He is currently an Associate Professor, an Assistant Director of Sakura Medical Center and a Head of the Department of Surgical Pathology at Toho University Sakura Medical Center, Chiba, Japan. He is also an Attending Scientist at the Cancer Institute, a Consultant for bone & soft tissue tumor pathology of National Cancer Center and Certified Pathologist of the Japanese Society of Pathology. His specialty is general surgical pathology and bone & soft tissue tumor pathology.